

Construction of a femtosecond laser for the study of aberrations in optical systems

Construcción de un láser pulsado en femtosegundos para el estudio de aberraciones en sistemas ópticos

Miguel Ángel González-Galicia*, M. Rosete-Aguilar*, J. Garduño-Mejía*, N. C. Bruce*, R. Ortega-Martínez*

ABSTRACT

We present the construction of a femtosecond laser, based on a titanium sapphire crystal. This laser produce pulses of 20 fs. We also present theoretical results for the electric field distribution near the focal plane of a lens for gaussian illumination under the influence of primary aberrations: spherical aberrations, coma, astigmatism and field curvature, for an achromatic doublet. The theoretical results are compared with results obtained with the laser system constructed.

RESUMEN

Presentamos la construcción de un láser pulsado en femtosegundos, basado en un cristal de titanio safiro. Este láser produce pulsos de 20 fs. También presentamos resultados teóricos para la distribución de campo eléctrico cerca del plano focal de una lente para iluminación gaussiana bajo la influencia de aberraciones primarias: aberración esférica, coma, astigmatismo y curvatura de campo, para un doblete acromático. Los resultados teóricos son comparados con los resultados experimentales obtenidos con el láser construido.

INTRODUCTION

The titanium sapphire laser $Ti : Al_2O_3$ is the most widely used tunable solid-state laser for femtosecond pulse generation. The emission wavelength range is 660 nm to 1180 nm (Silfvast, 2004). The main feature of this laser is its time resolution and the corresponding high peak powers, which makes the instrument suitable to produce nonlinear effects such as second harmonic generation, Stimulated Raman Scattering, Stimulated Brillouin Scattering, Self-Phase Modulation, Supercontinuum Generation, etc. The effect of the primary aberrations (spherical aberration, coma and astigmatism) on ultrashort pulses has been studied by Horváth, Kovács & Bor (2007) who applied the Nijboer-Zernike theory. In this paper we use the Seidel aberration theory for thin cemented lenses with the stop at the lens. The intensity of the pulse at the focal region of the lens in the presence of primary aberrations for a homogenous illumination beam incident on the lens is evaluated by using Kempe's approach, where the wave number is expanded up to second order (Kempe & Rudolph, 1992). We have added the effect of field curvature aberration in the wave aberration function. We present the real case, in which all aberrations are present.

The laser system

The laser system is a linear cavity, in which the active medium is a Titanium Sapphire crystal. It is pumped by a Verdi laser system, based on

Recibido: 10 de noviembre de 2012
Aceptado: 3 de junio de 2013

Keywords:

Láser pulsado; Ultrafast phenomena; femtosecond phenomena; Pulse compression; Pulses; Aberrations; lenses.

Palabras clave:

Láser pulsado; fenómenos ultrarrápidos; fenómenos de femtosegundos; pulsos; aberraciones, lentes.

*Centro de Ciencias Aplicadas y Desarrollo Tecnológico, Universidad Nacional Autónoma de México (UNAM). Circuito exterior s/n, Ciudad Universitaria, D.F., México. 04510. E-mail: miguel.gonzalez@ccadet.unam.mx; martha.rosete@ccadet.unam.mx; jesus.garduno@ccadet.unam.mx; neil.bruce@ccadet.unam.mx; roberto.ortega@ccadet.unam.mx

optically pumped semiconductor laser (OPSL) technology by Coherent Inc. at 532 nm. The pump beam is focused by a plano-convex lens. The pumping incident on the crystal surface. The crystal is cooled by water at a temperature of 18 °C. A pair of Fused Silica prisms is used to compensate the Group Velocity Dispersion produced by the crystal, the distance between prisms is 0.6 m. Fluorescence emitted by the crystal is collected within the cavity formed by mirrors E_1 , E_2 , E_3 , E_4 , E_5 and E_6 , as shown in figure 1. The lasing condition takes place when the gain exceeds the losses. The laser system begins to operate in continuous mode (CW) and under certain conditions can operate in a pulsed mode by a process known as Kerr-Lens-Mode Locking (KLML).

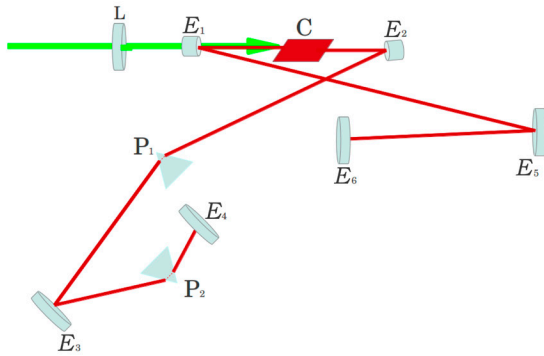


Figure 1. Linear cavity.
Source: Authors own elaboration.

The system is pumped to a power of 5 W and produces a pulse train at a frequency of 76 MHz. The average output power is 150 mW and the pulse duration is 20 fs. Beam size is 2.16 mm. Figure 2 shows the corresponding emission spectrum, while figure 3 shows the autocorrelation corresponding to 20 fs.

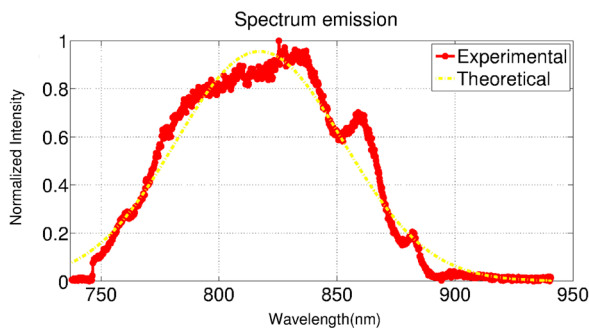


Figure 2. Emission spectrum.
Source: Authors own elaboration.

The temporal characterization of the pulses is performed with an autocorrelator based on a Michelson interferometer, the signal is detected with a photodiode which works due to the process of two-photon absorption. Beam spatial characterization is performed with the “Knife Edge” technique. The two measurements were taken along the focal plane.

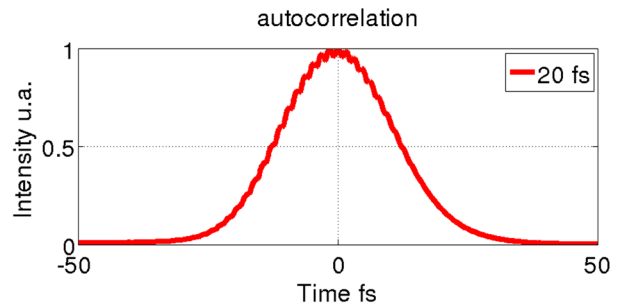


Figure 3. Autocorrelation.
Source: Authors own elaboration.

Diffraction theory

We define a pulse with a carrier wavenumber, $k_0 = \omega_0/c$, where ω_0 is the optical carrier frequency and c is the speed of light in vacuum. The wavenumber is defined as $k_a = k_0 (1 + (\Delta\omega/\omega_0))$ where $\Delta\omega = \omega - \omega_0$. The field distribution near the focal plane of lens can be estimated according to the following diffraction integral. The coordinate system is shown in figure 4.

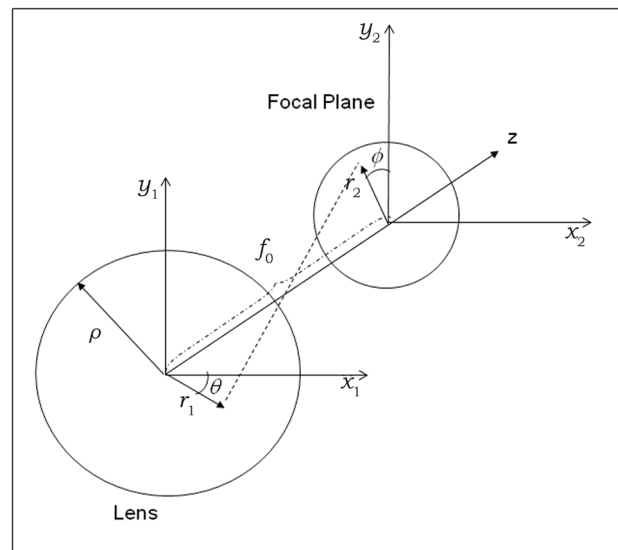


Figure 4. The coordinate system.
Source: Authors own elaboration.

$$U(x_2, y_2, z; \Delta\omega) \propto \int_{-\infty}^{\infty} \int_{-\infty}^{\infty} U_0(x_1, y_1, \bar{u}) P(x_1, y_1) A(\Delta\omega) e^{-i\Theta(x_1, y_1; \eta; \theta)} e^{i\phi(x_1, y_1)} \times e^{\frac{ik_0}{2z} [(x_2 - x_1)^2 + (y_2 - y_1)^2]} dx_1 dy_1. \quad (1)$$

where P is the pupil function given by

$$f(n) = \begin{cases} 1 & \text{if } x_1^2 + y_1^2 = r_1^2 \\ 0 & \text{if otherwise} \end{cases}, \quad (2)$$

ρ is the semidiameter of the lens. We assumed gaussian illumination so

$$U_0(x_1, y_1, \bar{u}) = e^{-\left[\frac{x_1^2 + y_1^2}{\omega_0^2}\right] \cos^2 \bar{u}} e^{i(k_0 y_1 \sin \bar{u})}, \quad (3)$$

where \bar{u} is the principal ray angle of the incident beam with respect to the optical axis of the lens measured in radians. $A(\Delta\omega)$ is a gaussian envelope input pulse given by

$$A(\Delta\omega) = A_0 \times e^{-\left[\frac{T\Delta\omega}{2}\right]^2}, \quad (4)$$

where T is half of the pulse width measured to $1/e$. The pulse intensity full width is given by $T_m = \sqrt{2}T$.

By introducing the variable chances

$$u = \rho^2 k_0 \left(\frac{1}{f_0} - \frac{1}{z} \right), \quad v = \frac{\rho k_0 r_2}{f_0} \quad \text{and} \quad N = \frac{\rho^2 k_0}{2f_0},$$

that the bandwidth is only a small fraction of the carrier frequency, *i.e.*, $\Delta\omega/\omega_0 \ll 1$ the field distribution near the focal plane of the lens is given by

$$U(u, v, \phi, \bar{u}, \Delta\omega) \propto e^{i[(k_1 d_1 + k_2 d_2)]} \int_0^1 r A(\Delta\omega) dr \times e^{-\frac{i}{2} \frac{u}{\omega_0^2}} \times e^{-\left[\frac{\rho^2}{\omega_0^2}\right] r^2 \cos^2 \bar{u}} \times e^{[-ir^2(\tau\Delta\omega + \delta\Delta\omega^2)]} \times e^{i(\tau r \Delta\omega + \delta \Delta\omega^2)} \times i \frac{v^2}{4N} \int_0^{2\pi} d\theta \times e^{(-iv \cos\theta(\theta - \phi))} \times e^{-i\Theta(r_1; \theta)} e^{ik_0 r_1 \cos\theta \sin \bar{u}}, \quad (5)$$

where

$$\tau = \frac{k_0 \rho^2}{2} \left(\frac{(n_1 - 1)b_1^1}{R_1} - \frac{(n_1 - 1)b_1^1}{R_2} + \frac{(n_2 - 1)b_2^2}{R_2} \right),$$

$$-\frac{(n_2 - 1)b_2^2}{R_3} - \left(\frac{k_0 \rho^2}{2f_0 \omega_0} - \frac{u}{2\omega_0} \right), \quad (6)$$

$$\delta = \frac{k_0 \rho^2}{2} \left(\frac{(n_1 - 1)b_1^1}{R_1} - \frac{(n_1 - 1)b_1^1}{R_2} + \frac{(n_2 - 1)b_2^2}{R_2} - \frac{(n_2 - 1)b_2^2}{R_3} \right), \quad (7)$$

$$\tau' = k_0 (n_1 d_1 a_1^1 + n_2 d_2 a_1^2), \quad (8)$$

$$\delta' = k_0 (n_1 d_1 a_2^1 + n_2 d_2 a_2^2). \quad (9)$$

By substituting the phase due to aberrations $\Theta(x_1; y_1; \eta; \theta)$ into equation (5), we have

$$U(u, v, \phi, \bar{u}, \Delta\omega) \propto e^{i[(k_1 d_1 + k_2 d_2)]} \times e^{-\frac{i}{4N}} \int_0^1 r A(\Delta\omega) dr \times e^{-\left[\frac{\rho^2}{\omega_0^2}\right] r^2 \cos^2 \bar{u}} \times e^{-ir^2(\tau\Delta\omega + \delta\Delta\omega^2)} \times e^{i(\tau r \Delta\omega + \delta \Delta\omega^2)} e^{-\left[-ik_0 \left(\frac{S_I}{8} r^4 + \frac{1}{4} (S_{III} + S_{IV}) r^2 \right) \right]} G(v, r, \phi, \bar{u}), \quad (10)$$

where

$$G(v, r, \phi, \bar{u}) = \int_0^{2\pi} e^{-iv \cos(\theta - \phi)} e^{-ik_0 \left(\frac{S_{II}}{2} r^2 \cos\theta + \frac{S_{III}}{2} r^2 \cos^2\theta \right)} \times e^{ik_0 \rho r \cos\theta \sin \bar{u}}. \quad (11)$$

The seidel coefficients are evaluated for the semidiameter of the lens.

In equation (11), if $\bar{u} = 0$, then $S_I \neq 0$, $S_I = S_{II} = S_{III} = S_{IV} = 0$ and $G(v, r, \phi, \bar{u}) = J_0(v, r)$.

The amplitude in the time domain is obtained by the Fourier transform of $U(u, v, \phi, \bar{u}, \Delta\omega)$:

$$U(u, v, \phi, \bar{u}, t) \propto \int e^{-i(\Delta\omega)t} U(u, v, \phi, \bar{u}, \Delta\omega) d\Delta\omega. \quad (12)$$

Collecting some common terms that multiply $\Delta\omega$ and $\Delta\omega^2$ and solving the integral over the frequency, the diffraction integral is given by

$$\begin{aligned}
 U(u, v, \phi, \bar{u}, t) \propto & K \int_0^1 \left(\frac{4\pi[1+i\varepsilon]}{T^2[1+\varepsilon^2]} \right)^{\frac{1}{2}} \times r dr \\
 & \times e^{-\frac{(t-r+r^2\tau+i\varepsilon)}{T^2[1+\varepsilon^2]}} e^{-i\left(\frac{u}{2}\right)r^2} \\
 & \times e^{-\left(\frac{\rho^2}{\omega_0^2}\right)r^2 \cos^2 \bar{u}} \\
 & \times e^{-ik_0 \left(\frac{S_{II}r^4 + \frac{1}{4}(S_{III} + S_{IV})r^2}{8} \right)} \\
 & \times G(v, r, \phi, \bar{u}), \quad (13)
 \end{aligned}$$

where

$$i\varepsilon = \frac{4i(\delta' - r^2\delta)}{T^2}. \quad (14)$$

Equation (13) gives the field distribution of the pulse near the focal plane of a lens when the wave-number is expanded up to the second order. To compare with experimental results, the spatial and temporal integrated quantities of $U(v, u; t)$ are determined as follows in equation (6) For the spatial profile

$$I(t) \propto \int_0^\infty [U(u, v, \phi, \bar{u}, t)]^2 v dv. \quad (15)$$

For the temporal profile

$$I(v) \propto \int_0^\infty [U(u, v, \phi, \bar{u}, t)]^2 v dt. \quad (16)$$

Theoretical and experimental results

The numerical model was solved for the real case, they appear all aberrations. For experimental results we proceeded to rotate the achromatic doublet a certain angle and get their respective autocorrelations. The spatial profile was obtained by the method of the “knife Edge”. Data were taken for 0°, 5° and 8°. The theoretical results are obtained by the following equations (González-Galicia, Rosete-Aguilar, Garduño-Mejía, Bruce & Ortega-Martínez, 2011b). The spatial and temporal axis in figures 5, 6, 7 and 8 are normalized quantities given by $v = pk_0 r_2 / f_0$ and

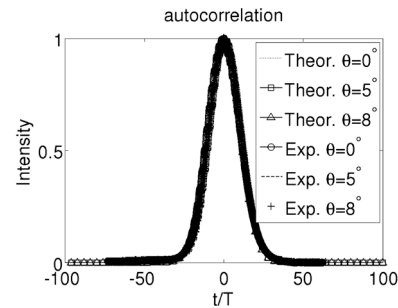


Figure 5. Autocorrelations.
Source: Authors own elaboration.

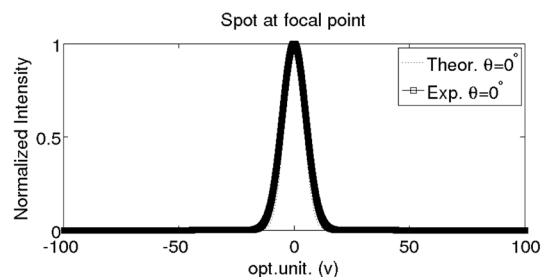


Figure 6. Experimental and theoretical beam spot measured at the focal plane for $\bar{u} = 0^\circ$.
Source: Authors own elaboration.

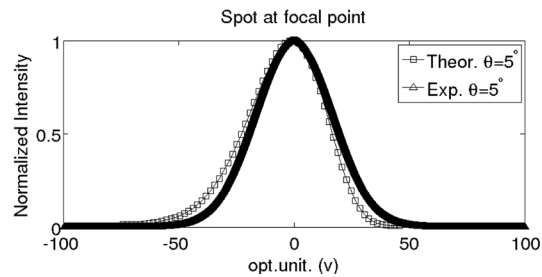


Figure 7. Experimental and theoretical beam spot measured at the focal plane for $\bar{u} = 5^\circ$.
Source: Authors own elaboration.

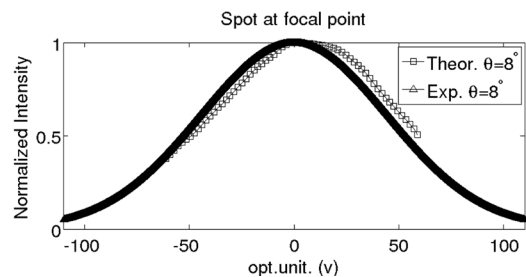


Figure 8. Experimental and theoretical beam spot measured at the focal plane for $\bar{u} = 8^\circ$.
Source: Authors own elaboration.

t/T_{int} . The achromatic doublet model is model NT45-794 from Edmund optics, with a focal length of 30 mm and a diameter of 12 mm.

CONCLUSIONS

We have evaluated the field distribution near the focal plane of a lens for gaussian illumination, where are all aberrations. No temporal distortion occurs when rotating the achromatic doublet. By comparing the experimental results and the theoretical results obtained from autocorrelations, we find that the two results agree. Spatial distortion increases as the value of the angle is rotated the achromatic doublet.

ACKNOWLEDGMENTS

Miguel Ángel González Galicia acknowledges that this work would not have been possible without a grant from *Coordinación de Estudios de Posgrado, Universidad Nacional Autónoma de México* (UNAM). He would also like to thank to the *Secretaría de Educación Pública-Subsecretaría de Educación Superior-Dirección General de Educación Superior Universitaria* project 2012-01-21-002-205 and *Consejo Nacional de Ciencia y Tecnología* (Conacyt) project 00000000189688 for supporting the LAOP Workshop 2012, where this work was presented. The

authors acknowledge the Office of Research and Postgraduate Support (*Dirección de Apoyo a la Investigación y Posgrado*, DAIP) of the University of Guanajuato for the editing of the English-language version of this paper. *Dirección General de Asuntos del Personal Académico-Universidad Autónoma de México*, (DGA-PA-UNAM) (PAPIIT- IN104112) (PAPIIT RR181212) y Conacyt, (CB2009 No. 1311746).

REFERENCES

- González-Galicia, M. A., Rosete-Aguilar, M., Garduño-Mejía, J., Bruce, N. C. & Ortega-Martínez, R. (2011)a. Effects of primary spherical aberrations, coma, astigmatism and field curvature on the focusing of ultrashort pulses: homogeneous illumination. *Journal of the Optical Society of America. A*, 28(10), 1979-1989.
- González-Galicia, M. A., Rosete-Aguilar, M., Garduño-Mejía, J. Bruce, N. C. & Ortega-Martínez, R. (2011)b. Effects of primary spherical aberrations, coma, astigmatism and field curvature on the focusing of ultrashort pulses: gaussian illumination and experiment. *Journal of the Optical Society of America. A*, 28(10), 1990-1994.
- Kempe, M. & Rudolph, W. (1992). Spatial and temporal transformation of femtosecond laser pulses by lenses and lens systems. *Journal of the Optical Society of America B*, 9(7), 1158-1165.
- Horváth, Z. L., Kovács, A. P. & Bor, Z. (2007). Distortion of ultrashort pulses caused by aberrations. *Springer Series in Chemical Physics*, 88, 220-222.
- Silfvast, W. T. (2004). *Laser Fundamentals*. United Kingdom: Cambridge University Press.